Electronic Supplementary Material (ESI) for Physical Chemistry Chemical Physics.

ESI for "Photoluminescence study of time- and spatial-dependent light induced trap de-activation in $CH_3NH_3PbI_3$ perovskite films"

Xiao Fu*, Daniel A. Jacobs, Fiona J. Beck, The Duong, Heping Shen, Kylie R. Catchpole and Thomas P. White

Centre for Sustainable Energy Systems, Research School of Engineering, Australian National University, Canberra, 2601 Australia.

*Email: xiao.fu@anu.edu.au

Fig. S1 shows the image of perovskite film captured by Scanning Electron Microscope (SEM). The average crystal size is around 200 nm.

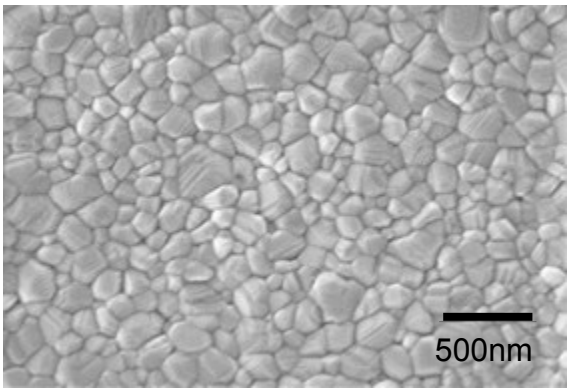

Fig. S1 SEM image of perovskite film

Fig. S2 demonstrates a representative IV curve of the planar perovskite cells produced with the same film fabrication process as used in this work. The inset table indicates the figures of merit of this cell.

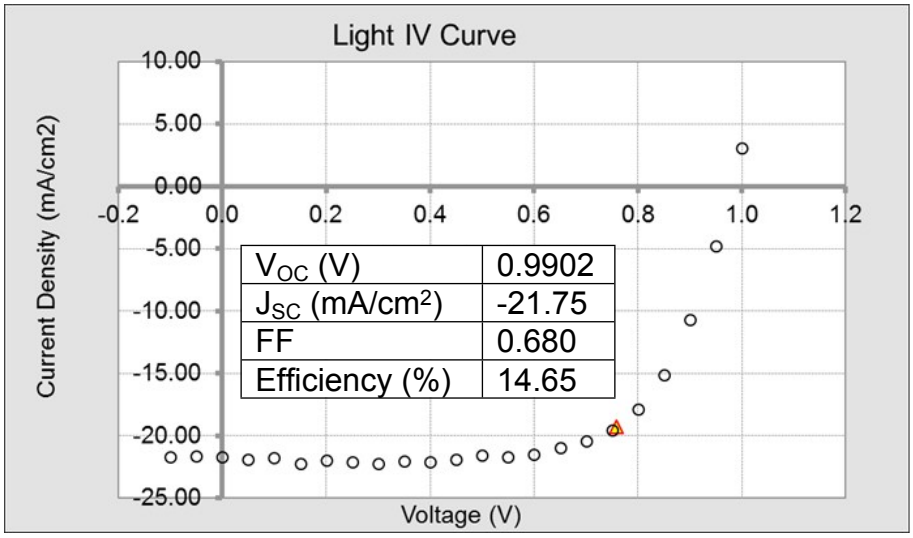

Fig. S2 IV curve of planar perovskite cell. The inset table shows the performance parameters of this cell.

According to the equation $Spot\ Size = \frac{1.22 \cdot \lambda_{EX}}{NA}$, the calculated minimum laser spot size are 2.163 μm for Olympus MPlanFL N 10× lens and 0.763 μm for Olympus MPlanFL N 100× lens.

Fig. S3a and S3b are the CDD camera captured images of the fine focused laser spots on double side polished Si wafer. Fig. S3c and S3d are the cross section plots of the laser spots. We obtain spot sizes of 8.25 μm and 0.926 μm respectively for the 10× and 100× objective lenses by fitting to a Gaussian profile.

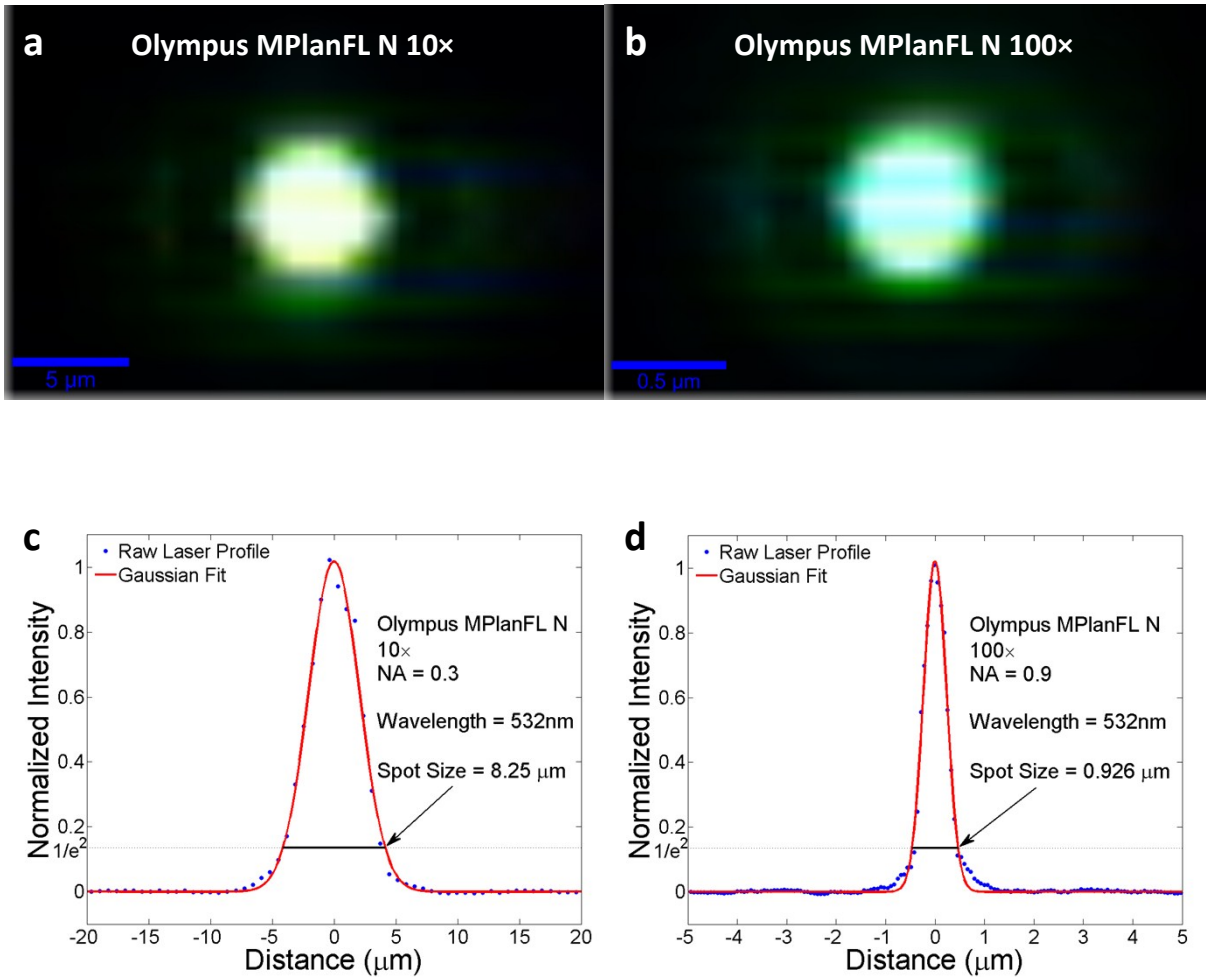

Fig. S3 Images of laser spot captured by CCD camera using (a) Olympus MPlanFL N 10× objective lens and (b) Olympus MPlanFL N 100× objective lens. (c) and (d) are the cross section plots of the Gaussian beam shown in (a) and (b) respectively.

Fig. S4 shows the comparison of the light induced PL changes on a bare perovskite film and a film coated with PMMA. It indicates that PMMA can protect perovskite films from degradation for the duration of the measurement.

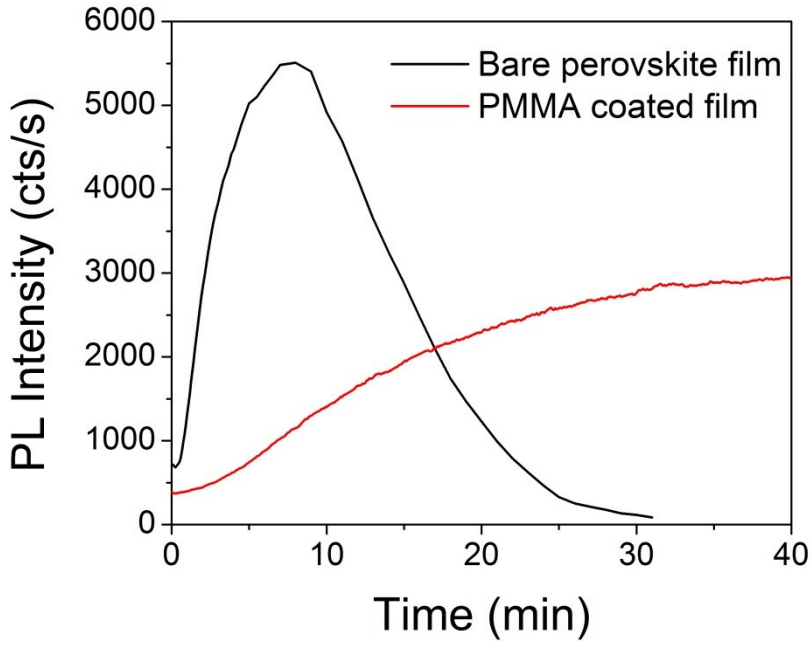

Fig. S4 Time-resolved PL changes of a bare perovskite film (black) and a film coated with PMMA (red).

Fig. S5 shows the comparison of the light induced changes on a PMMA coated perovskite film and a fully encapsulated perovskite film. It indicates that PMMA does not completely block the perovskite film from air.

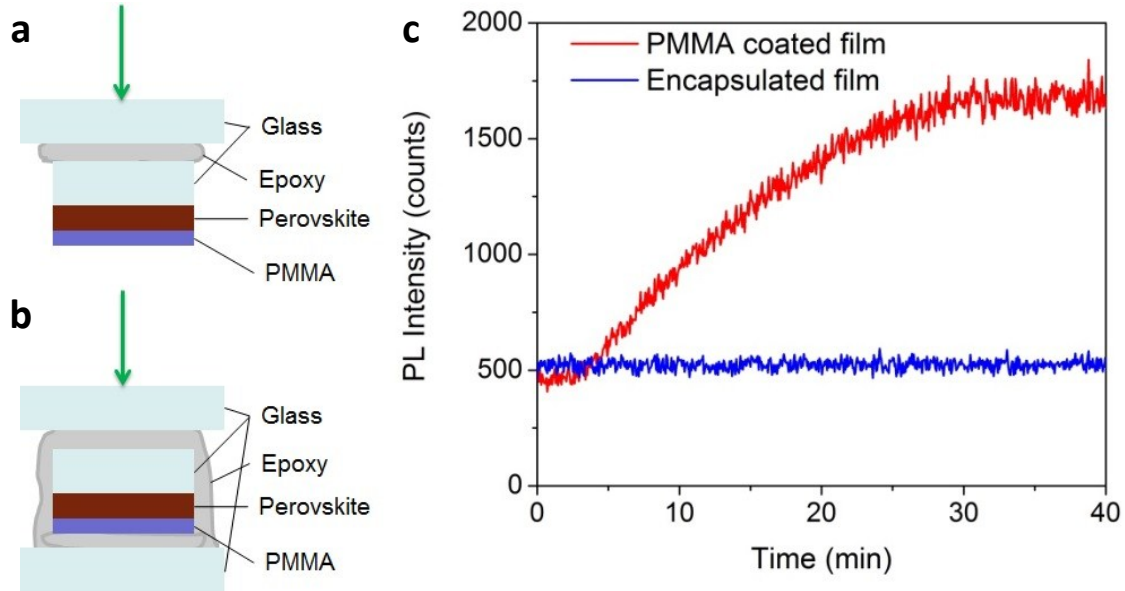

Fig. S5 Schematic diagram of (a) PMMA coated perovskite film and (b) fully encapsulated perovskite film in this experiment. (c) Time-resolved PL changes of the two type of films under same test condition. The

red line indicates a PL increase of the PMMA coated film with laser illumination; the blue line shows that the PL intensity of the encapsulated film does not change.

With constant trap density N_T, it only takes 10μs for the PL enhancement to saturate (Fig. S6a). The rapid PL increase depends purely on trap filling. If we fit the time scale with the experimental result in Figure 1b, all the rates should be reduced by more than ten orders of magnitude. These values are far below reasonable trapping, de-trapping and recombination rates for perovskite films (Fig. S6b). This result suggests that trap filling alone cannot explain the experimentally observed PL changes.

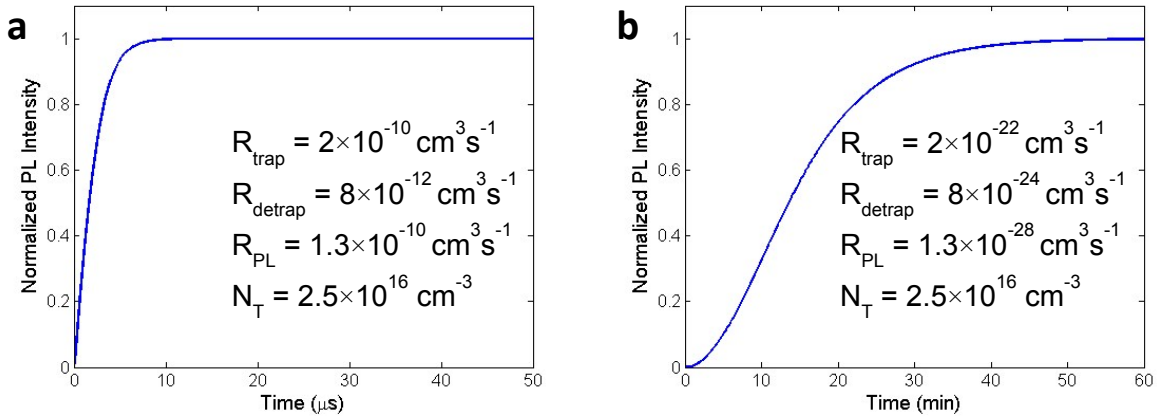

Fig. S6 Modelled PL increase with constant trap density (a) using reasonable rates and (b) using rates that can fit the measured timescale.

Fig. S7 shows the modelled PL enhancement variation with incident power for a single set of fitting parameters.

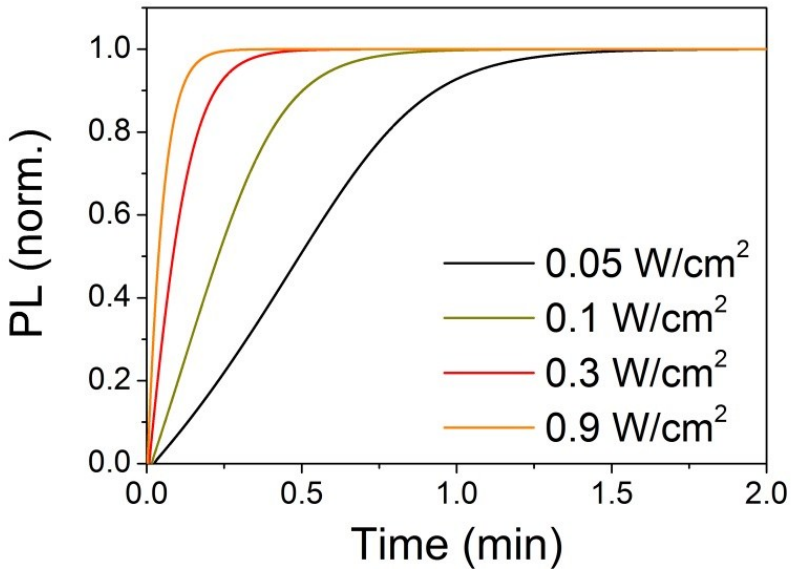

Fig. S7 Modelled power-dependent PL increase as a function of time.

Fig. S8 shows that if the pre-illuminated sample is stored in an N_2 environment in the dark for a sufficiently long time (>30min), the PL intensity will drop to the original level.

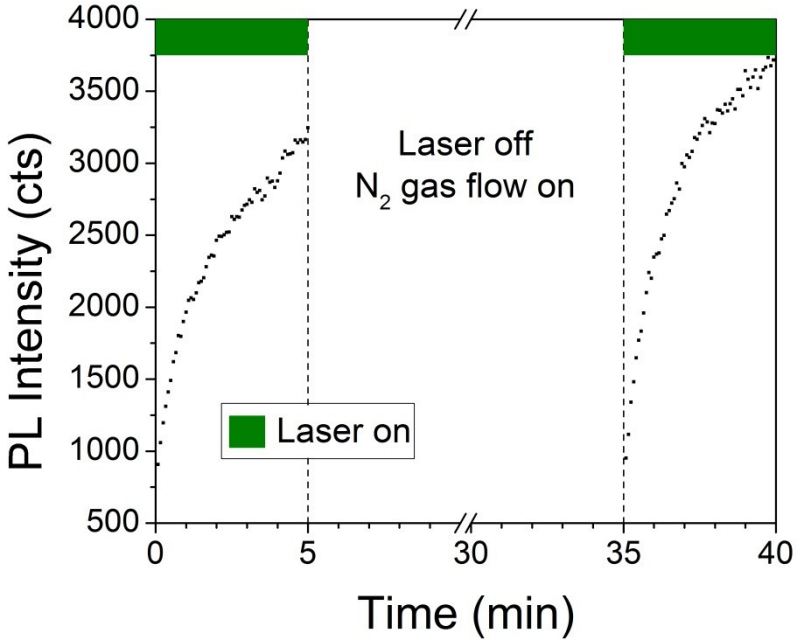

Fig. S8 Single point PL intensity measurement with intervals of laser exposure.

The semiconductor model developed for this study incorporated the 2-dimensional semiconductor drift-diffusion equations (although no electric field was present for the drift contribution) plus terms accounting for generation and recombination via traps, as well as radiative recombination. The semiconductor module of COMSOL Multiphysics was used to solve these equations for an input trap density profile which was determined by the competition between de-activation via free electrons and re-activation on a preset timescale:

$$\frac{\partial N_t}{\partial t} = -R_{deac} n_e N_t + \frac{N_{t0} - N_t}{\tau_{reac}} \qquad (1)$$

Starting from a trap distribution with uniform density N_{t0}, the semiconductor model was used to determine n_e, which was then used to update the trap distribution according to (1) ready for input into the semiconductor module at the next timestep. After generating a history of trap densities we performed a simulation of the PL imaging process in a fully 2-dimensional model which accounted for the finite laser spot size and the focal width, both of which were found to be significant given the rapid spatial variation in recombination rates.

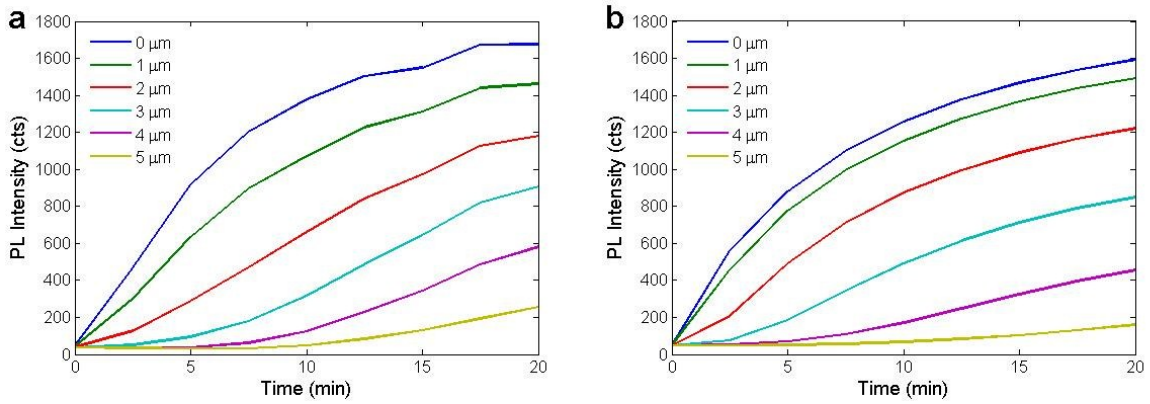

Fig. S9 Line plots of the averaged PL data at varying displacements from the central spot for (a) experimental and (b) modelled results.

Table S1 Parameters used in the semiconductor model.

N_{t0} (initial trap density)	$2 \times 10^{10}\ cm^{-3}$
C_n,C_p (capture probabilities)	$3 \times 10^{-10}\ cm^{-3} s^{-1}$
R_{deac} (rate of trap de-activation)	$2 \times 10^{-16}\ cm^{3} min^{-1}$
τ_{reac} (timescale of trap re-activation)	$20\ min$
E_t (defect level)	$0.7\ E_g$
μ_n,μ_p	$4\ cm^{3} V^{-1} s^{-1}$
P_{soak}/P_{probe}	$130 W cm^{-2}/80 W cm^{-2}$
d_{soak}/d_{probe}	$2.1 \mu m/0.7 \mu m$
C (radiative coefficient)	$1.7 \times 10^{-10}\ s^{-1} cm^{-3}$

In Fig. S10a we show that our model is able to reproduce the qualitative trend reported in Fig. 3 of the main text, in which the PL enhancement was shown to accelerate after recovering periods when the laser was switched off. This can be understood by inspection of Fig. S10b which shows that the most significant recovery after switching off the illumination occurs in the central region, whereas the de-activation “progress” further away is almost unaffected. After the recovery period a high photogenerated carrier density is able to rapidly de-activate the central region once more to resume the de-activation of defects at the expanding boundary.

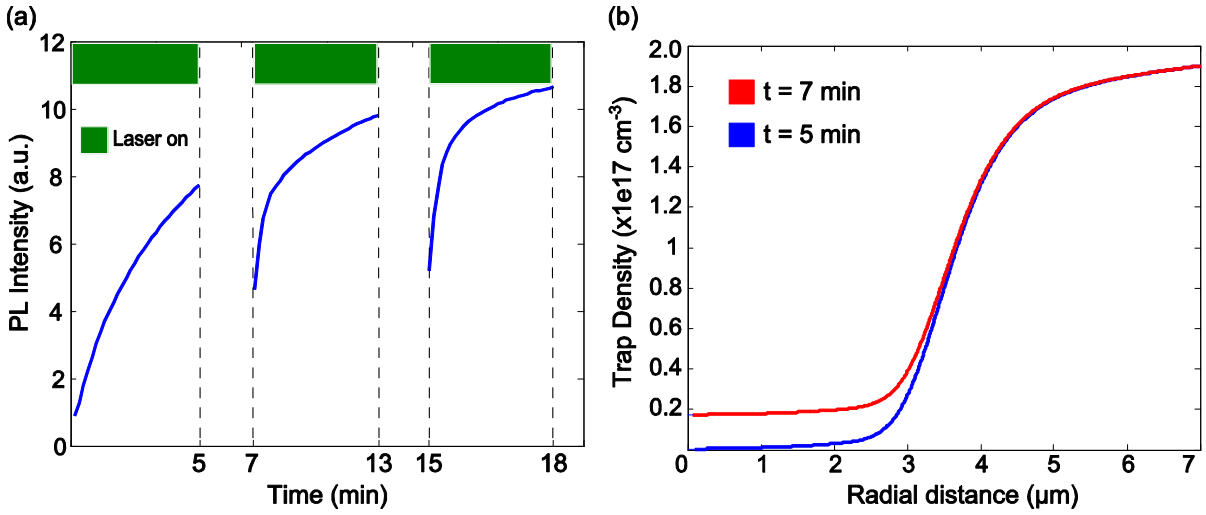

Fig. S10 (a) Simulated PL intensity following periods when the illumination is switched off and traps are allowed to recover. (b) Trap densities immediately before and after the recovery period beginning at t=5min showing a rapid recovery in the central region where the density of de-activated traps is largest.